JOURNAL OF MATERIALS SCIENCE **39** (2004) 557–564

Influence of the shape of fiber cross section on fabric surface characteristics

M. A. BUENO
Ecole Nationale Supérieure des Industries Textiles de Mulhouse (College of Textiles), University of Mulhouse, 11 rue Alfred Werner-68093 Mulhouse, France
E-mail: ma.bueno@uha.fr

A. P. ANEJA
E.I. DuPont de Nemours and Company, Dacron Research Laboratory, Kinston, N.C. 28501, USA
E-mail: Arun-Pal.Aneja-1@usa.dupont.com

M. RENNER
Ecole Nationale Supérieure des Industries Textiles de Mulhouse (College of Textiles), University of Mulhouse, 11 rue Alfred Werner-68093 Mulhouse, France
E-mail: m.renner@uha.fr

Fiber cross sections for use in textiles and composites are becoming more and more complex. Shape impacts fiber or filaments properties and therefore the yarn and fabric characteristics. This paper presents the influence of the fiber cross section on the fabric surface characteristics. The material used was polyester staple fibers, of four different shapes: round, scalloped oval, cruciform and hexachannel. All fibers had the same cut length with different fineness. Yarns obtained from these fibers had nominally the same yarn count, torsion value and structure. Plain jersey fabrics were knitted from each of the yarns under identical conditions and then relaxed prior to testing. Friction behavior was evaluated and a roughness-friction criterion developed. An indirect measurement of the real area of contact was obtained in order to provide roughness and friction properties. The influence of fiber cross section on yarn bending rigidity and on the state of the knitted fabric surface was characterized. © *2004 Kluwer Academic Publishers*

1. Introduction

Today, round fiber cross section is the most common shape manufactured by synthetic fiber producers. Other shapes are beginning to emerge for a variety of reasons—performance, comfort, pilling propensity, bulkiness, tactility, processing, etc. [1–3]. In the present article we will analyze the contribution of the shape of fiber cross section on fabric surface physical characteristics.

For a study of this kind, all variables must be kept constant with the exception of the one parameter whose influence is being evaluated. Hence, to study the contribution of the fiber cross section on fabric properties only cross section must vary. Previous investigators in their analysis of the impact of fiber cross section on fabric parameters have ignored this critical aspect [4, 5]. In fact, while changing cross section other parameters like fiber fineness [5] or yarn linear density and number of warp and weft threads per unit length [6] were also altered. Others have changed the cross section with a view to imitate natural fiber tactility [3, 7].

There are many critical properties of the fabric which are impacted by the shape of the fiber cross section. Bulk, crease recovery, flexural rigidity, abrasion resistance, pilling, handle, luster, dyeing are just a few of the properties which the consumer must consider in his decision making for the choice of a garment. No particular cross section has all the desired features for every consumer. One of the most important advantages to be achieved in the use of modified cross-section fibers is perhaps in the flexural rigidity. Varying degrees of fabric softness, drape, crispness and stiffness are possible with fiber cross section.

The aim of this paper is to study the influence of the shape of fiber cross section on the yarn behavior and the knitted fabric surface state. All fabrics tested were constructed under identical conditions of spinning and knitting. The state of fabric surface was evaluated by two techniques: a tribological one and a measurement of the real contact area between the fabric and a smooth plate. Both methods indicate the importance of fiber cross section on the knit fabric relief. The contribution of fiber cross section is explained at the fiber, yarn and fabric scale.

TABLE I Fiber characteristics

Fiber set	Mass per unit length in dtex (10^{-4}g·m^{-1})	Cross section	Non-roundness factor (κ)	Moment of inertia ((10^{-6} m)^4)	Tenacity (10^{-3} N·dtex^{-1})
Fine	1.58	Round (R)	1.02	1992	28.3
	1.75	Scalloped oval (SO)	1.25	1410	21.0
	2.04	Cruciform (C)	1.52	4145	15.4
Coarse	3.39	Round (R)	1.02	9285	23.7
	4.18	Scalloped oval (SO)	1.27	8043	18.2
	4.32	Hexachannel (H)	1.57	8439	12.9

2. Experimental

2.1. Material

Fibers were melt-spun with the same molecular weight (LRV 9.3) [8] polyester (PET) (Table I). Four different fiber cross sections, each with varying fineness, i.e., mass per unit length were obtained. Two sets, one of lower fineness (from 1.6 to 2 dtex, where 1 dtex represents 10^{-4} g·m^{-1}) of round, scalloped oval and cruciform shape and the other of coarse fineness (from 3.4 to 4.3 dtex) of round, scalloped oval and hexachannel shape (Fig. 1) were manufactured. All had identical manufacturing process conditions except for the spinneret; each cross section had a specially designed spinneret. The fiber area and perimeter were measured using a Hardy plate dry technique. These quantities were measured for five different filaments in the bundle and the average obtained. These values were used to calculate the "non-roundness" factor κ defined below (Table I):

$$\kappa = \frac{C_f}{2\sqrt{\pi S}} \tag{1}$$

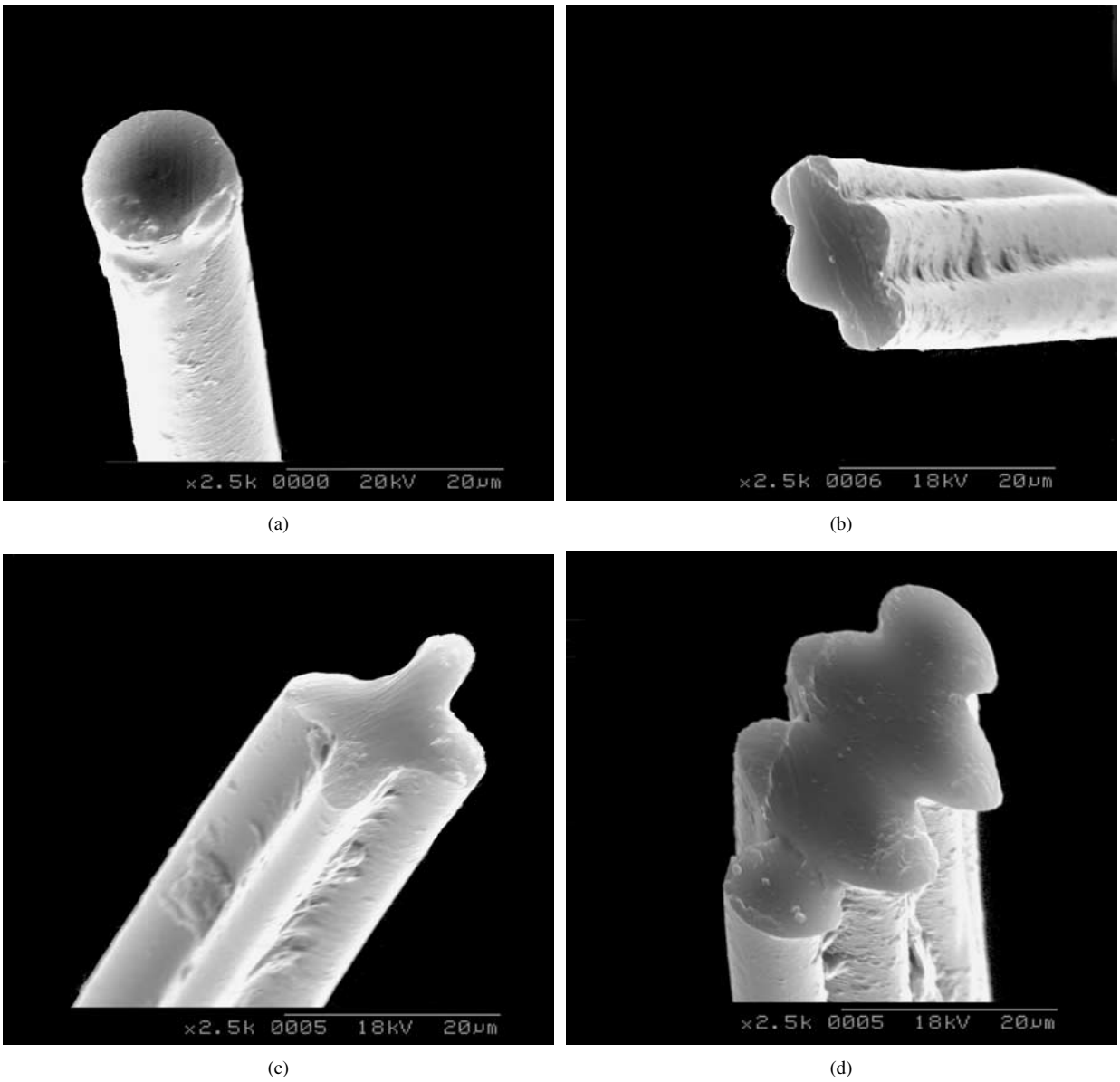

(a) (b) (c) (d)

Figure 1 Fiber shapes photographs.

TABLE II Yarn characteristics

Fiber set	Fiber	Yarn mass per unit in tex (10^{-3} g·m^{-1})	Yarn torsion (twist per meter)
Fine	R 1.58 dtex	35.8	573
	SO 1.75 dtex	36.0	576
	C 2.04 dtex	36.5	579
Coarse	R 3.39 dtex	35.0	593
	SO 4.18 dtex	36.4	585
	H 4.32 dtex	36.5	569

where, κ, non-roundness factor (dimensionless); C_f, fiber circumference (m); S, fiber cross-sectional area (m^2).

The value of κ depends only on filament shape, not on size. The minimum possible value of $\kappa = 1$ is achieved with a round fiber shape. Since there is some fineness variability in the bundle, the measured κ value for different items of the same shape were not exactly equal to each other, as they should have been. The value reported in the table is averaged over the various items with the same cross-section shape.

All fibers have a length of about 40 mm. Yarns were made using a ring spinning process. They all have the same structure, yarn count and torsion (Table II). Plain jersey fabrics were knitted with a loop length of 0.5 cm, with identical machine settings.

Knitted fabrics are easy to deform hence it is impossible to know their state of deformation. Therefore in order to test knitted fabric in a reproducible way, fabric had to be relaxed. After relaxation, the yarn and the fabric are both at a minimum internal energy state. Knitted fabrics consist of loops in three-dimension conformation which explains their important property of deformability (Fig. 2). The loop characteristics represent a balance between inter-yarn friction forces and yarn bending rigidity. For hydrophilic fabrics, like polyester, relaxation consists of a mechanical process of agitation in presence of heat. The aim is to impart energy to the system in order to counter the friction inter-yarn forces. The process of relaxation ceases when the friction forces and yarn bending forces are in equilibrium. Thus, during knitting the fabric is stressed in the wale direction (axis-y) by the take-down system, while during relaxation the fabric retracts in the same direction (Fig. 3).

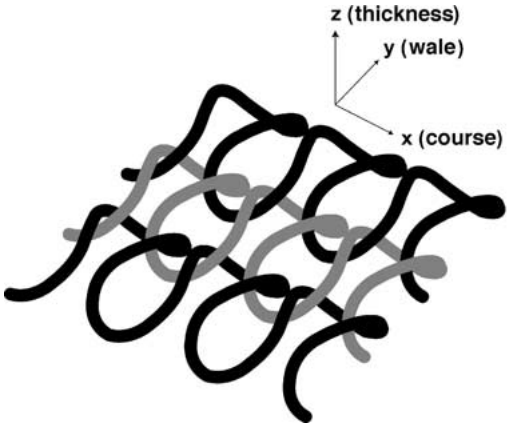

Figure 2 Three-dimensional loop shape in a weft knitted fabric.

We can compare two fabrics knitted under identical conditions; one which has been manufactured with a flexible yarn, the other with a more rigid yarn. The yarn bending rigidities are respectively B_f and B_r, with $B_f < B_r$.

After relaxation, two possibilities exist relative to inter-yarn friction force, F_f and F_r respectively.

When $F_r < F_f$, the fabric made with the more flexible yarn will retract but will retain its elongation in the wale-wise direction. The fabric will also remain more flattened, i.e., smooth. For fabric made from a rigid yarn, the result will show a more significant retraction in the wale direction. Therefore, after full relaxation, the flexible yarn will give a smoother surface than the rigid one. In addition, the 3D loop shape of a relaxed fabric will depend on the tension of the take-down system. Thus, when the yarn is more flexible and the inter-yarn friction force is higher, the fabric is more sensitive to the take-down tension.

When $F_f < F_r$, retraction after relaxation is similar for both fabrics and will have similar surface roughness. Retraction is equally significant for fabrics made with more flexible yarn. Hence, differences between both fabrics are less important than the previous case. The contribution of take-down tension is less important.

2.2. Measurement methods used

Measurement methods have been described in a previous paper [9]. Here, we will explain them briefly.

2.2.1. Indirect technique to assess the real contact area

The real contact area has been defined [10] as the contact area between the top of the asperities of two surfaces (Fig. 4). Usually, this area is much smaller than the apparent area of contact. Therefore, the mean pressure is much lower than the real pressure at the contact points. From that real area of contact, friction properties and surface roughness can be characterized as follows:

$$F = A \cdot s \tag{2}$$

where, F, friction force (N); A, real contact area (m^2); s, frictional shear stress (Pa).

Moreover,

$$W = P_m \cdot A \tag{3}$$

where, W, normal load (N); P_m, real pressure (Pa).

When the real contact area between a rough and a smooth surface is measured, it results in the characterization of surface roughness of the rough surface. Therefore, in order to define the fabric surface state, the real contact area between the knitted fabric and a smooth plate is measured. The smooth plate surface consists of a polished aluminum surface.

An apparatus was developed to assess the real contact area by an indirect technique. The method measures the transient heat conduction in a vacuum. Transient heat conduction is transfer of thermal energy due to

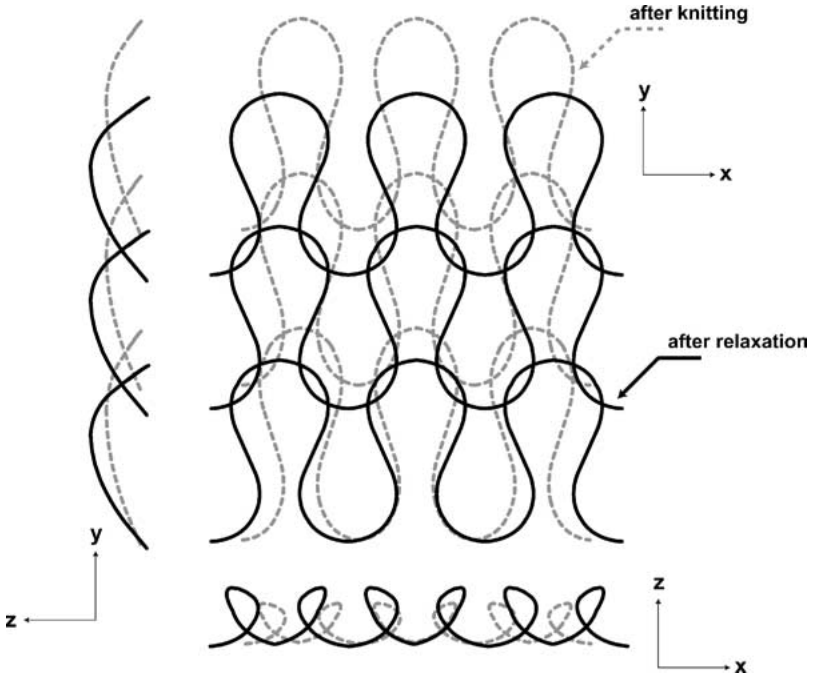

Figure 3 Weft-knitted fabric after knitting process and after relaxation.

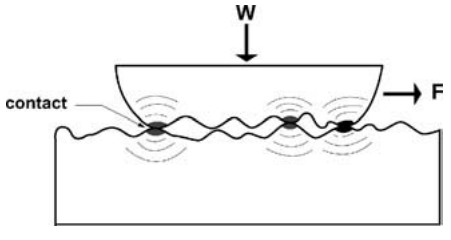

Figure 4 Contact between two surfaces occurs on the top of the asperities.

molecular interactions under a non-homogeneous temperature distribution. Heat conduction requires contact between surfaces. For identical materials increasing the area of contact increases the conduction phenomenon. Furthermore, when the real contact area is large, the material absorbs more energy. The energy absorbed by the system is proportional to the real area of contact shown below:

$$\frac{E}{\Delta t} = \lambda A \frac{\Delta T}{e} \tag{4}$$

where, E, energy absorbed by the system (J); Δt, time of the measurement (s); λ, thermal conductivity of the material in the heat flow direction ($W \cdot m^{-1} \cdot K^{-1}$); A, real area of contact (m^2); ΔT, difference of temperature (K) between the hot plate and the ambient; e, fabric thickness (m).

For homogeneous materials, Equation 4 indicates that for a given temperature gradient, energy absorbed by the system increases with increasing thermal conductivity of the material; the fabric thickness is supposed to be constant. Thus, more a material absorbs thermal energy during contact by conduction, the superior are its conductive properties with heat flow in normal direction to the surface.

$$\vec{\varphi} = -\lambda \vec{\nabla} T \tag{5}$$

where, the heat flow is in the normal direction to the surface: $\vec{\varphi}$, heat flow density in normal direction of the surface ($W \cdot m^{-2}$); λ, thermal conductivity of the material in the heat flow direction ($W \cdot m^{-1} \cdot K^{-1}$); T, time-dependent temperature field (K).

For a fibrous material, the thermal conductivity is a combination of thermal conductivity of the air and that of the fiber (weighted respectively by the fraction of the volume taken up by each component). However, in the present case, the fabric is in a vacuum. The contribution of air in the fabric is negligible and the most significant effect is the conductivity of fibers.

In order to measure the thermal energy absorbed by a fabric, an apparatus consisting of a guarded hot plate shown in Fig. 5 was developed. It has a square, thin central aluminum test plate (100 mm^2-area) surrounded by a coplanar ring aluminum plate (292 mm^2-area). The central plate and the guard ring are separated by a thin polystyrene band (2 mm-width). They are heated by two independent cemented resistances heater wires. The ring plate is at a temperature of 0.5°C higher than the test plate, i.e., 33.5°C, to avoid lateral heat loss from the central test plate and prevent any heat transfer from ring plate to the test plate.

After bringing the test plate and the guard ring plate to the desired operating temperature, 33 and 33.5°C, respectively, it is necessary to wait until equilibrium is reached between the system and the ambient environment. At the equilibrium state, the electrical power supplied by the resistances remains constant. At this point, the fabric sample is placed on the surface of the test plate. There is an instantaneous heat loss by the plate and a temperature gradient exists through the fabric. The electrical power as a function of time required by the system (plate plus sample) to reach 33°C again is recorded. Since the guard ring avoids any lateral heat loss, the measurement reflects the vertical heat flow between the test plate and the sample. The thermal

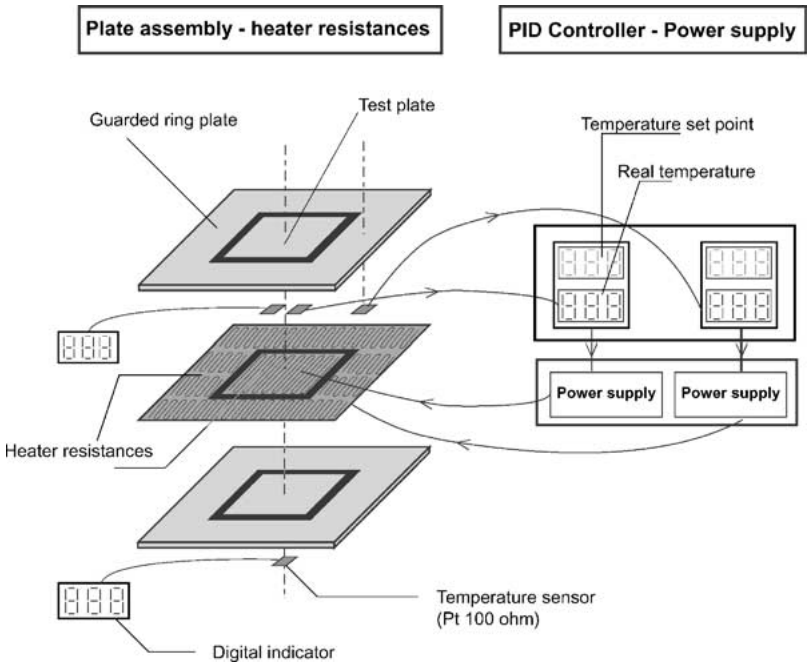

Figure 5 Apparatus for real contact area measurement.

energy lost by the test plate is equal to the energy absorbed by the fabric plus a constant C_1. The heat flow to the test plate is equal to the electrical power supplied by the heater wire resistances plus a constant C_2. The constants C_1 and C_2 are independent from the fabric. They only depend on the imposed temperature gradient ΔT. In our study, this gradient is constant and equal to 13°C, i.e., the temperature difference between the atmosphere temperature (20°C) and the operating temperature (33°C).

Under these conditions, the thermal energy transferred to the fabric is the difference between the power measured at the equilibrium state without the sample and the power measured with a sample on the test plate. The thermal energy, absorbed by the sample is calculated by multiplying instantaneous power absorbed by the fabric during the time interval. Hence, it is very important to have a short time interval (less than one second, in our case 0.8 s). At a steady state (longer time interval), the energy absorbed is mostly due to the raw material and not the structure or the real area of contact.

2.2.2. Technique to assess fabric surface roughness-friction

A multi-directional tribometer is used for this measurement. It consists of three parts: drive for the sample, sensor and a signal-processing unit (Fig. 6). The sample carrier is a 140-mm diameter rotary disk. The sensor is positioned at one end of a balance arm with counterweight at the other. This arm is fixed on the frame that supports the sample carrier. The sensor is a piezoelectric accelerometer. The probe attached to the sensor is a steel wire (0.5 mm in diameter and 5 mm in length) with its axis radial to the sample carrier. The surface to be scanned is a rotary disk of 110-mm diameter. Measurements are performed at a rotation speed of 0.258 rps (linear speed of 89 mm·s^{-1}).

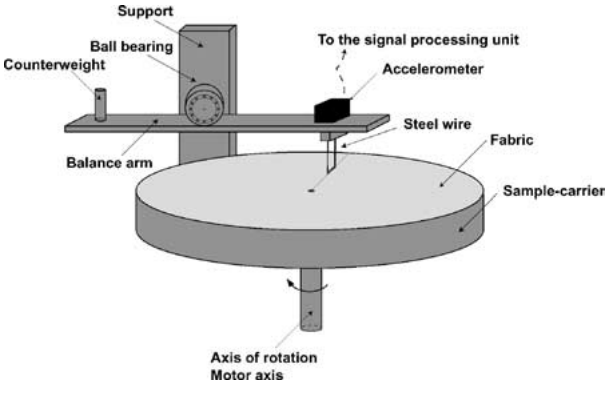

Figure 6 Tribometer for roughness-friction criterion measurement.

The Fourier analysis of the electrical signal from the sensor consists of computing the autospectrum relative to frequency by a spectrum analyzer. The autospectrum is the average of several instantaneous spectra during sample carrier rotation. Each spectrum is expressed in power spectral density (PSD) relative to frequency. The power spectral density is obtained as follows:

$$\mathrm{PSD}(f) = \frac{|X(f)|^2}{K * \Delta f} \tag{6}$$

where, f, frequency (Hertz, Hz); $X(f)$: Fourier transform of the temporal signal $x(t)$, which corresponds here to the signal from the sensor (m·s^{-2}); PSD, power spectrum density ((m·s^{-2})^2·Hz^{-1}); Δf, step in frequency domain, $\Delta f = 1$ Hz; K, coefficient relative to the windowing (dimensionless). In our case, we used a Hanning window, then $K = 1.5$.

All fabrics have a periodic structure based on the basic pattern (kind of weave or knit). Thus, the power spectral density shows one or several peaks corresponding to the periodicity of the fabric structure. The number of peaks is equal to the number of periodicity scanned

by the probe during sample rotation. For jersey fabrics, the power spectral density has one peak which corresponds to the wales.

The frequency value of each peak is equal to:

$$f = \frac{\pi D \omega}{l} \tag{7}$$

where, D, diameter of the scanned surface (m); ω, rotation speed (rps); f, frequency (Hz); l, length of a spatial period (m).

A spatial period shows the distance between two asperities (in our case two wales of the knitted fabric).

The height of the frequency peak corresponding to this spatial period evolves in the same direction as the friction force due to these asperities. This friction force depends on the height of the asperities and the material. Hence, for a given material, the peak maximum is obtained by the asperity height. This defines the fabric surface roughness. The asperity height is governed by the yarn undulation in the fabric. Hence, rougher the structure, the higher is the frequency peak maximum. This parameter is called roughness-friction criterion.

3. Results and discussion

3.1. Results

As indicated previously, we obtained data on two sets of fibers. One group consists of round, scalloped oval and cruciform shapes with nominal mass per unit length 1.8 dtex. The other group consists of round, scalloped oval and hexachannel with a nominal fineness of 3.9 dtex. The bending rigidity of a fiber relative to an axis δ, approximated as a beam, is [11]:

$$B = E \cdot I \tag{8}$$

where, B, bending rigidity relative to the axis δ ($\mathrm{N \cdot m^2}$); E, Young modulus of the material ($\mathrm{N \cdot m^{-2}}$); I, moment of inertia of the cross section relative to the axis δ ($\mathrm{m^4}$).

Therefore for a given material, the bending rigidity is determined by the moment of inertia. It was calculated for each fiber relative to an axis δ based on the equation indicated below [12]:

$$I_{\mathrm{fiber}_{\mathrm{axis}\delta}} = \frac{\eta}{4 \cdot 10^{20} \cdot \pi \cdot \rho_{\mathrm{f}}^2} \cdot t_{\mathrm{f}}^2 \tag{9}$$

or

$$I_{\mathrm{fiber}_{\mathrm{axis}\delta}} = \frac{\eta}{4 \cdot \pi} \cdot S^2 \tag{10}$$

where, η, shape factor, equal to 1 for a circular fiber (dimensionless); ρ_{f}, fiber density ($\mathrm{g \cdot cm^{-3}}$); t_{f}, fiber mass per unit length (dtex $= 10^{-4} \mathrm{g \cdot m^{-1}}$); S, fiber cross-sectional area ($\mathrm{m^2}$).

The fabric properties of friction-roughness criterion obtained by the tribometer and the real contact area by the thermal device in vacuum were measured for the fine (Fig. 7) and coarse (Fig. 8) fibers (Table I).

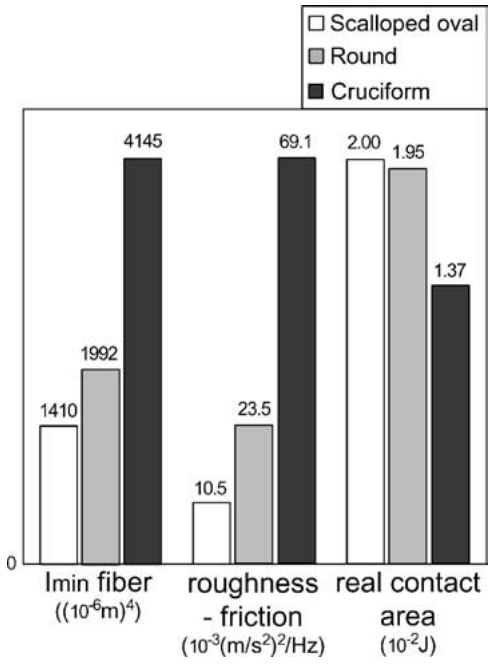

Figure 7 For fine fiber set: minimum moment of inertia, roughness-friction criterion and real contact area.

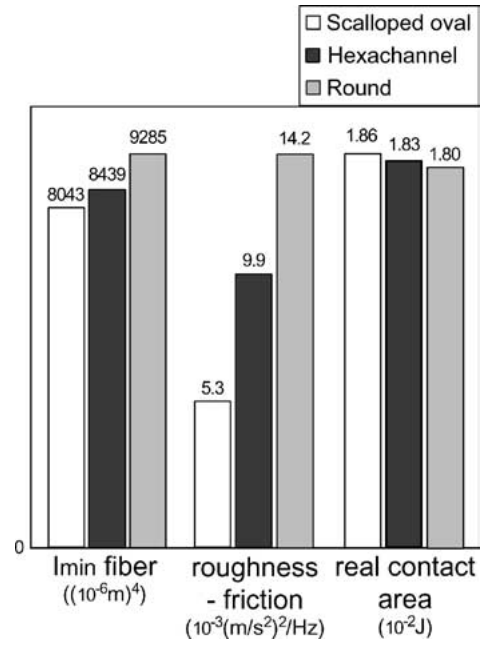

Figure 8 For coarse fiber set: minimum moment of inertia, roughness-friction criterion and real contact area.

3.2. Discussion

As indicated previously (Equation 8), the bending rigidity of a yarn for a given material depends on the moment of inertia of the yarn, and hence on the moment of inertia of each fiber relative to axis Δ. This is defined as the yarn axis with lower bending rigidity (Fig. 9). The governing equation is:

$$I_{\mathrm{yarn}_{\mathrm{axis}\Delta}} = \sum I_{\mathrm{fiber}_{\mathrm{axis}\Delta}} \tag{11}$$

where, $I_{\mathrm{yarn}_{\mathrm{axis}\Delta}}$, moment of inertia of the yarn relative to the axis Δ ($\mathrm{m^4}$); $I_{\mathrm{fiber}_{\mathrm{axis}\Delta}}$, moment of inertia of each fiber relative to the axis Δ ($\mathrm{m^4}$).

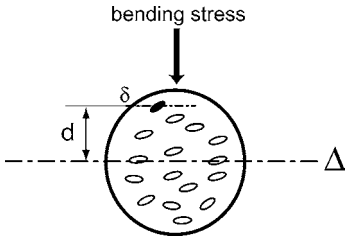

Figure 9 Yarn made from fibers under bending stress.

According to Huyghens theorem [11], the moment of inertia of each fiber relative to axis Δ of the yarn, shown in Fig. 9, depends on the moment of inertia of each fiber relative to its axis δ and the corresponding distance to the yarn axis Δ.

$$I_{\text{fiber}_{\text{axis}\Delta}} = I_{\text{fiber}_{\text{axis}\delta}} + S \cdot d^2 \tag{12}$$

where, $I_{\text{fiber}_{\text{axis}\delta}}$, moment of inertia of a fiber relative to its axis δ (m^4); S, cross-section area of the fiber (m^2); d, distance between axis Δ and δ (m).

Since, all yarns have identical structure, yarn count and torsion value, it is assumed they have the same yarn cross-sectional area. For each set of fiber fineness, the yarns have the same number of fibers in the cross section. Hence, the moment of inertia of each yarn is governed by the fiber moment of inertia. With increasing fiber moment of inertia, it is expected that the yarn moment of inertia will increase. As indicated previously, relaxation of fabric plays a dominant role in yarns with higher bending rigidity. This results in a higher contribution from retraction forces resulting in fabrics of rougher tactility. This was confirmed by the experiments as shown in Figs 7 and 8. In these figures, we observe that with increasing fiber moment of inertia a corresponding rise in friction-roughness criterion. This is true for both sets of fibers of low and high mass per unit length. We also observed that with increasing moment of inertia the real contact area decreases.

With increasing fiber fineness (Equations 9–12) and hence decreasing fiber moment of inertia, one would expect the fabric friction-roughness criterion to increase. This was not observed for round and scalloped oval shapes (Figs 10 and 11). Increasing fiber mass per unit length increases yarn hairiness (Table III) because of increased fiber mass moment of inertia *Im* relative to the yarn axis *D* [1]:

$$Im_{\text{fiber}_{\text{axis}D}} = \int r^2 \cdot dm \tag{13}$$

Where, $Im_{\text{fiber}_{\text{axis}D}}$, fiber mass moment of inertia relative to the axis *D* ($m^2 \cdot kg^{-1}$); *D*, yarn axis; *r*, distance between a fiber element and the axis *D* (m); *dm*, mass of a fiber element (kg).

TABLE III Yarn hairiness index

Fiber shape	Fiber fineness (dtex)	Yarn hairiness index (m of hairs per m of yarn)
Round	1.58	7.07
	3.39	8.66
Scalloped oval	1.75	8.24
	4.18	9.55

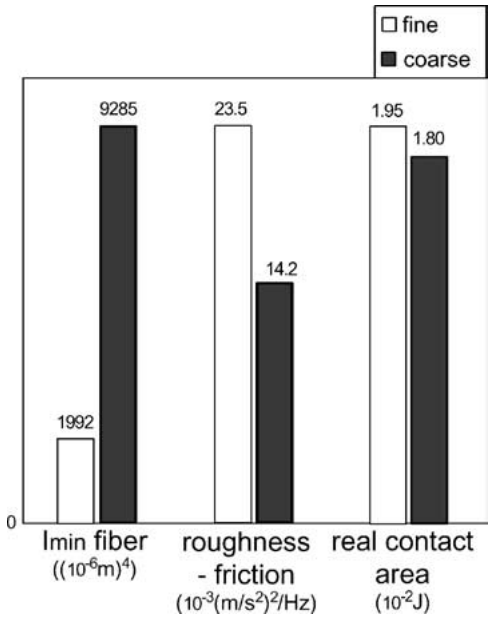

Figure 10 For round fibers: minimum moment of inertia, roughness-friction criterion and real contact area.

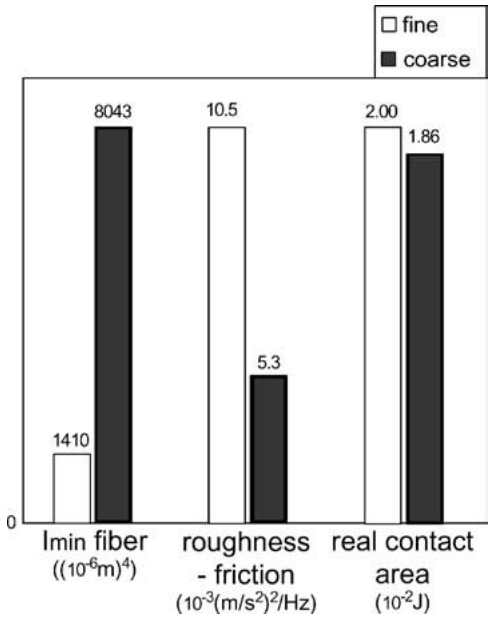

Figure 11 For scalloped oval fibers: minimum moment of inertia, roughness-friction criterion and real contact area.

For a fixed distance *r*, increasing fiber mass per unit length increases the mass moment of inertia. Hence, coarse fibers have increased propensity to protrude from the yarn surface as hair.

Yarn hairiness can mask the contribution of the stitch relief for a knit structure. This results in lower fabric friction-roughness criterion from the tribometer than in the absence of hairiness. Also, the real contact area decreases with increasing hairiness.

A fiber defined as hair is not contained in the yarn cross section, hence it is free. During bending, it tends to move towards the axis Δ. The distance *d* decreases (Equation 12, Fig. 12) resulting in lower yarn moment of inertia for a hairy yarn than for a non-hairy yarn made from identical fibers. Hence, decreasing the yarn

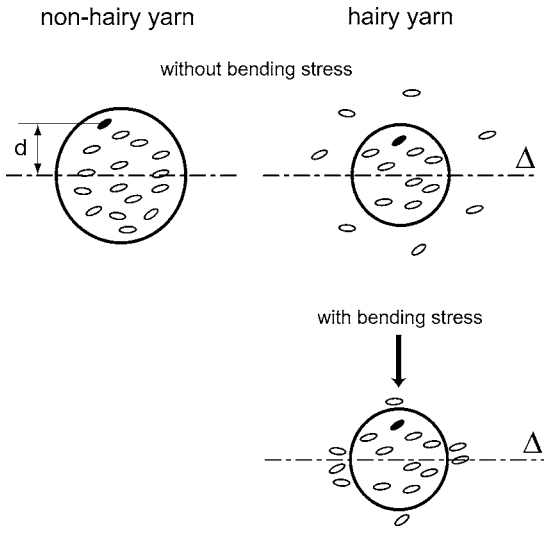

Figure 12 Hairy yarn made from fibers under bending stress.

moment of inertia due to hairiness has a more significant impact than that of increasing moment of inertia due to increased fiber mass per unit length. Yarns made from coarse fibers are less rigid than the yarn made with fine fibers. Hence, for coarse fibers, the fabric friction-roughness criterion is low and the real contact area is high.

Figs 10 and 11 show that with coarse fibers, the fabric friction-roughness criterion and the real contact area are lower than with finer fibers. Therefore, in that case the most important contribution is not the difference in moment of inertia between yarns made with coarser or fine fibers but the level of hairiness.

4. Conclusion

Fibers with four different shapes (round, scalloped oval, cruciform and hexachannel) were evaluated in this study. In addition we studied two sets of fiber fineness. The results indicate that increasing moment of inertia, as governed by the shape of fiber cross-section, leads to a corresponding increase in the fabric friction-roughness criterion coupled with decrease in the real contact area. Furthermore, the contribution of the fiber moment of inertia to the yarn bending rigidity and the knitted loop structure is explained.

With increasing fiber fineness one would expect the moment of inertia to decrease resulting in a smoother fabric. However, we did not observe this trend. Yarns made from coarse fibers result in higher level of hairiness, thus reducing the contribution of fiber mass per unit length. This resulted in higher fabric roughness-friction criterion and an increase in real contact area for fine fibers.

In order to have the softest fabrics based on the shape of the fiber, it is necessary to have the lowest moment of inertia. This may be achieved by decreasing fiber mass per unit length or by designing a desired shape of fiber cross section. The moment of inertia of the fiber should be low in one direction relative to the axis. Consequently, it is high in the transverse direction as is, for example, the case for a ribbon or in the limit a "line" shape fiber. For this shape, the "non-roundness" factor κ becomes very large, approaching infinity. This shape poses a problem during arrangement of fibers in the yarn cross section. All fibers must bend in the direction of their minimum moment of inertia. This is not possible with a ribbon or a "line" shape. One way to overcome this for a twisted "line" shape fiber is to have incremental twists small enough to allow each fiber to bend in the direction of its minimum moment of inertia in the yarn structure. Such a fiber would give the smoothest knitted fabrics for a given stitch length.

Acknowledgment

Appreciation is expressed for the cooperation Dr. Marie-José PAC during her PhD thesis.

References

1. W. J. MORRIS, *Text. Mag.* **18** (1989) 2.
2. M. OKAMOTO and K. KAJIWARA, Papers Presented at the World Conference (1995) p. 348.
3. O. WADA, *J. Text. Inst.* **83** (1992) 322.
4. R. K. DATTA, A. M. SHAH and N. C. PATEL, *ATIRA Comm. Text.* **29** (1995) 146.
5. M. MATSUDAIRA, Y. TAN and Y. KONDO, *J. Text. Inst.* **84** (1993) 373.
6. M. MATSUDAIRA, *ibid.* **83** (1992) 24.
7. M. FUKUHARA, *Text. Res. J.* **63** (1993) 387.
8. C. BROADDUS, "Batts and Articles of New Polyester Fiberfill," U.S. Patent no. 5,104,725 (1991).
9. M.-A. BUENO, M. RENNER and M.-J. PAC, *J. Mater. Sci.* **37** (2002) 2965.
10. F. P. BOWDEN and D. TABOR, "Ch. 3: Adhérence, endommagements des surfaces et mécanisme de la friction" (Monographies Dunod, Paris, 1959) p. 22.
11. J. M. DATAS, "Ch. 2: Propriétés géométriques des sections" (Cépaduès-Editions, Toulouse, 2001) p. 16.
12. W. E. MORTON and J. W. S. HEARLE, "Ch 17: Forces in Various Directions" (The Textile Institute, Londres, 1975) p. 399.
13. M. R. SPIEGEL, "Ch. 9: Mouvements plans des solides indéformables" (McGraw-Hill, Paris, 1972) p. 224.

Received 16 October 2002
and accepted 25 August 2003